

Composition-Dependent Morphological Transition of Hierarchically-Ordered Structures Formed by Multiblock Terpolymers

Jun Masuda,[†] Atsushi Takano,[†] Jiro Suzuki,[‡] Yutaka Nagata,^{†,§} Atsushi Noro,[†] Kennichi Hayashida,[†] and Yushu Matsushita^{*,†}

Department of Applied Chemistry, Graduate School of Engineering, Nagoya University, Furo-cho, Chikusa-ku, Nagoya 464-8603, Japan, The Computing Research Center, High Energy Accelerator Research Organization, 1-1 Oho, Tsukuba 305-0801, Japan

Received January 19, 2007; Revised Manuscript Received March 10, 2007

ABSTRACT: Morphological transition of two types of multiblock terpolymers with composition has been investigated. One is undecablock terpolymers of the PISISISIP type, while the other is hexablock terpolymers of the PISISI type, where P, I, and S denote poly(2-vinylpyridine), polyisoprene, and polystyrene, respectively. These polymer samples were prepared on the basis of anionic polymerization method. The volume fractions of P, ϕ_P , of the former are 0.08, 0.21, 0.53, whereas those of the latter are 0.64, 0.75, and 0.87. Nanophase-separated structures were observed by TEM and SAXS, and it was confirmed that their hierarchical morphology transforms from spheres-in-lamellae structure into cylinders-in-lamellae, lamellae-in-lamella, and coaxial cylindrical structures and finally into onionlike spherical structure with increasing volume fraction of the P component. From these results, it has been found that morphological transition of multiblock terpolymers takes place obeying conventional rule, i.e., the domain shape of P component varies as sphere–cylinder–lamella–matrix as ϕ_P increases with keeping hierarchical lamellar structure from I and S.

I. Introduction

Nanophase-separated structures of block copolymers have been extensively studied both theoretically and experimentally for this last four decades. Among the polymers with various architectures, AB diblock copolymers have been most frequently investigated and structural features have been clarified most precisely so far. For example, they tend to change their morphologies depending on volume fractions of component polymers,^{1,2} their periodic domain sizes increase with the molecular weight of the constituent polymers,^{3,4} and furthermore their morphological transition takes place depending on environmental conditions such as temperature and pressure and so on.^{5,6}

Morphologies of more complex systems were studied in turn. Among them, many equilibrium structures were observed for ABC triblock terpolymers having various compositions^{7,8} and block chain lengths,^{9,10} while theoretical works predicted various stable structures under given conditions.^{11,12} The other various complex systems, such as ABA triblock copolymers,^{10,13,14} AB₂ graft copolymers,^{10,15,16} star-shaped molecules of the (AB)_n type,^{17,18} (AB)_n multiblock copolymer systems,^{19–21} AB ring-shaped copolymers,^{22,23} and ABC star-shaped terpolymers,^{24–26} were also widely studied.

Recently the researches on hierarchical structures with mesoscopic and multiple length scales have been focused. Polymeric materials with double periodicity were introduced by ten Brinke et al.,^{27–29} while Asari et al. found the hierarchical lamellar structures with two different periodicities for complex AB or ABA and CD block copolymer blend systems with

hydrogen bonding.^{30,31} However, the directions of the different periodicities in hierarchical lamellar structures observed in these studies are perpendicular each other.

The materials with two quite different periodicities along the same direction can be conceived to be a useful photonic crystal.³² Nagata et al. prepared and characterized a styrene (S)–isoprene (I) undecablock copolymer having long S chains on two ends with nonablock copolymer of the (IS)₄I type at the center.³³ It was confirmed this undecablock copolymer forms a three-layered lamellae-in-lamella structure, i.e., a hierarchical lamellar structure, composed of one thick lamellar domain formed by two long S chains and I–S–I three thin lamellar domains. Recently, simulations for complex multiblock copolymers were performed by ten Brinke and co-workers,^{34–36} and various structures were predicted depending on molecular parameters defined and Flory–Huggins interaction parameter between component polymers. Furthermore, bulk structure of undecablock terpolymer having long poly(2-vinylpyridine) (P) chains on two ends with (IS)₄I nonablock copolymer at the center was observed most recently,³⁷ and “five-layered” lamellae-in-lamella structure composed of one thick P lamella and I–S–I–S–I five thin lamellae was reported. In addition the long-range ordering of the five-layered lamellar structure is very high because of two competing interactions over different length scales.

Composition dependence on three-phase hierarchical structures of multiblock terpolymers, particularly focusing on the chain length of the third component, has never been explored and it must be an interesting issue. This paper, therefore, has picked up this topic and observed three-phase complex structures for two series of multiblock terpolymers composed of I, S, and P polymers. One is the undecablock terpolymer series of the type P(IS)₄IP with relatively low volume fraction of P component and the other is the hexablock terpolymer series of the type P(IS)₂I with higher volume fraction of P. Their nanophase-separated structures were observed by TEM and SAXS methods

* Corresponding author: E-mail: yushu@apchem.nagoya-u.ac.jp. Telephone: +81-52-789-4604. Fax: +81-52-789-3210.

[†] Department of Applied Chemistry, Graduate School of Engineering, Nagoya University.

[‡] The Computing Research Center, High Energy Accelerator Research Organization.

[§] Present address: JSR Corporation, 5–6-10, Tukiji, Tyuo-ku, Tokyo 104-0045, Japan.

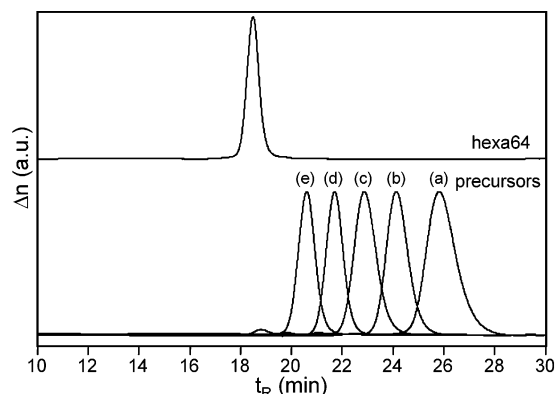
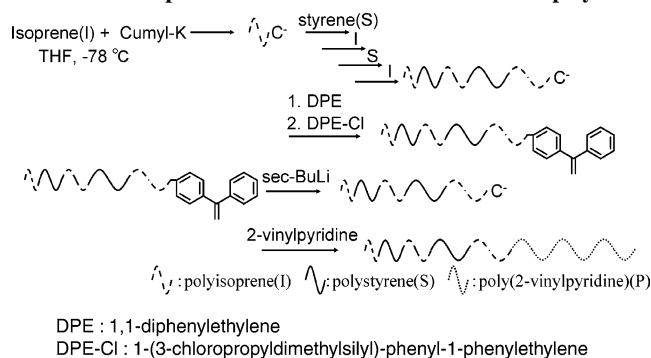


Figure 1. Comparison of GPC chromatograms of five precursors: (a) I, (b) IS, (c) ISI, (d) ISIS and (e) ISISI, and hexa64.

Scheme 1. Preparation Scheme of ISP Hexablock Terpolymers



complementally, and the morphological transition of three-phase hierarchical structures with the volume fraction of component P has been reported.

II. Experimental Section

Preparation and Characterization of Terpolymers. Undecablock and hexablock terpolymers composed of poly(2-vinylpyridine) (P), polyisoprene (I), and polystyrene (S) were prepared and used. The details of synthesis of an undecablock terpolymer were denoted in a previous work.³⁷ Two hexablock terpolymers were synthesized by sequential anionic polymerizations of isoprene and styrene resulting in producing a pentablock terpolymer of the ISISI type, followed by end capping with functional double bond leading polymerization of 2-vinylpyridine. The synthetic procedure of hexablock terpolymers is schematically shown in Scheme 1. Small amount of solutions were isolated in the course of polymerization so as to keep the common precursors for characterization. The samples were purified by fractionation using a gel permeation chromatography (GPC) with SC-8020 of Tosoh Corp. at room temperature. Molecular weight distribution of the purified products was also estimated by GPC system, HLC-8020 of Tosoh Corp. at 40 °C, and all runs for GPC measurements were made in THF containing 1% *N,N,N',N'*-tetramethylethylenediamine (TMEDA) as an eluent. Figure 1 compares GPC chromatograms of a hexablock terpolymer and those of their precursors as an example. It is evidently recognized that all the precursors and the final block terpolymer are monodisperse reflecting successful anionic polymerizations followed by careful purification by GPC. All the other samples were confirmed to be monodisperse polymers though their chromatograms are not shown here. Chemical compositions of samples were measured by 500 MHz ¹H NMR, Varian INOVA. Molecular weights of ISP undecablock and hexablock terpolymers were estimated by using the weight fractions of polystyrene and polyisoprene in terpolymers determined by ¹H NMR and molecular weights of the precursors. The sample codes, i.e., undecaX and hexaX are used to express two series, where undeca and hexa denote the numbers of block chains and X represents volume percent of P

Table 1. Molecular Characteristics of Undecablock Terpolymers and Those Precursors

sample	$M_w \times 10^{-4}$	M_w/M_n^a	ϕ_S^d	ϕ_I^d	ϕ_P^d
ISI	4.14 ^b	1.06	0.63	0.37	
ISISI	7.71 ^b	1.06	0.38	0.62	
ISISISI	10.2 ^b	1.07	0.55	0.45	
ISISISISI	14.4 ^b	1.07	0.42	0.58	
undeca8	15.8 ^c	1.08	0.39	0.53	0.08
undeca21	18.9 ^c	1.05	0.34	0.45	0.21
undeca53	33.9 ^c	1.03	0.21	0.26	0.53

^a Determined by GPC (1 vol % TMEDA/THF) ^b Determined by MALLS
^c Calculated by M_w of the previous precursor and weight fraction estimated by ¹H NMR ^d Determined by ¹H NMR

Table 2. Molecular Characteristics of Hexablock Terpolymers and Those Precursors

sample	$M_n \times 10^{-4}$	M_w/M_n^a	ϕ_S^b	ϕ_I^d	ϕ_P^d
I	6.14 ^b	1.09			
IS	18.5 ^c	1.05	0.64	0.36	
ISI	27.3 ^c	1.06	0.42	0.58	
ISIS	47.0 ^c	1.04	0.65	0.35	
ISISI	61.5 ^c	1.04	0.49	0.51	
Hexa64	190 ^c	1.02	0.16	0.20	0.64
Hexa75b	281 ^c		0.11	0.14	0.75
Hexa87	544 ^c	1.02	0.06	0.07	0.87

^a Determined by GPC (1 vol % TMEDA/THF). ^b Determined by ¹H NMR. ^c Calculated by M_n of the previous precursor and weight fraction estimated by ¹H NMR.

component. Table 1 shows the molecular characteristics of three undecablock terpolymers and their common precursors. From Table 1, it is apparent that the volume percent of P component is increasing from top to bottom, and these results ensure that three ISP undecablock terpolymers having nine short block chains of S and I at the center of the molecules and two P block chains on both ends have been prepared quite successfully as designed. Table 2 shows the molecular characteristics of two hexablock terpolymers together with their common precursors. It should be noted in this table hexa75b is the blend sample from the hexablock terpolymer and a P homopolymer ($M_w = 29.1$ K, $M_w/M_n = 1.02$).

Morphological Observation. Sample films for morphological observation were prepared by solvent casting from dilute solution of THF; the experimental details were described in a previous work.³³ As-cast films were dried well in a vacuum oven, followed by annealing at 150 °C for 6 days.

For transmission electron microscopy (TEM) experiments, the ultrathin sections were cut off from film specimens by an ultramicrotome, Reica Ultracut UCT, and a diamond knife. In order to enhance contrast, the ultrathin sections of sample films were stained with osmium tetroxide (OsO_4) and/or iodine (I_2). It is known that when the ultrathin sections are stained with OsO_4 and I_2 , the I, S, and P domains give strong, light and intermediate contrasts, respectively, in transmission electron micrographs, while the contrast for P domain is enhanced if I_2 only is used as a staining agent. The TEM instrument used was HITACHI H-800, operated under the acceleration voltage of 100 kV.

Small-angle X-ray scattering (SAXS) measurements were performed to observe nanophase-separated structures, compensatively. The instrument used was the apparatus installed in the beamline 15A at the Photon Factory in Tsukuba equipped with an X-ray imaging plate. The camera length, L (mm), and the wavelength of the X-ray beam, λ (nm), were ca. 2.3 m and 0.150 nm. X-ray beam was irradiated from the edge direction, where incident X-ray are parallel to the film surface. Another SAXS measurement using a microbeam SAXS apparatus was performed to observe nanophase-separated structure in local area using the instrument installed at the high flux beamline BL40XU at SPRING-8 facility in Hyogo equipped with a helical undulator. The camera length and the wavelength of X-ray beam is ca. 3.0 m and 0.1181 nm, respectively. The details of the microbeam SAXS measurements were described in a previous work.³⁸ For microbeam SAXS measurements, the

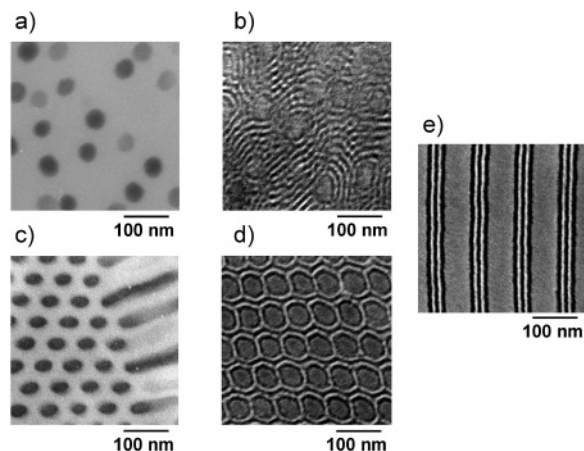


Figure 2. Transmission electron micrographs of undeca8 (a, b), undeca21 (c, d), and undeca53 (e). Ultrathin sections were stained with I_2 (a and c) and OsO_4 and I_2 (b, d, and e).

sample films were cut into thin sections with ca. 30 μm thicknesses by the ultramicrotome.

III. Results and Discussion

The precursors for undecablock terpolymers were confirmed to show lamellar structures except the triblock copolymer, which exhibits a bicontinuous structure (see the Supporting Information). The domain spacing of the nonablock copolymer, i.e., the longest precursor, was determined to be 16.9 nm.

Figure 2 shows transmission electron micrographs of three undecablock terpolymers. From Figure 2, parts a and b, it is evident that undeca8 forms spheres-in-lamellae structure with spheres of P component embedded in matrix of multilayered S-I lamellae. However the ordering of sphere is very low probably because of strong and frustrated strain of S and I chains as matrix. The domain spacing of the layered matrix of S and I is estimated to be ca. 17 nm from the transmission electron micrograph in Figure 2b, and its value is close to that of the nonablock copolymer. From Figure 2c for undeca21 stained with I_2 , P component forms ordered cylindrical structure in S-I matrix. Furthermore, as is clearly seen in Figure 2d, the matrix is finely phase separated into thinner five layers composed of I and S aligned alternatively. Thus, it is confirmed undeca21 forms cylinders-in-lamellae structure with hexagonally aligned cylinders of P component in matrix of five-layered S-I lamellae. As was reported previously,³⁷ undeca53 shows lamellae-in-lamella structure consisting of one thick P lamella and five thin I-S-I-S-I lamellae as in shown in Figure 2e; it has two crystallographic periods, i.e., 88 and 16 nm.

Microbeam SAXS was performed to observe more detailed nanophase-separated structure for local area of undeca21. Figure 3a shows a microbeam SAXS pattern, where the white arrows are the scattering vectors, $q_{(10)}$ and $q_{(01)}$, and the corresponding two vectors **a** and **b** in real space are superimposed on a transmission electron micrograph of undeca21 as shown in Figure 3b. In the SAXS pattern, spotlike reflections are observed, indicating that the X-ray beam size is small enough to probe only a limited number of periodic cells ordered hexagonally in the sample film. From this SAXS pattern, $|q_{(10)}|$ and $|q_{(01)}|$ were determined to be 0.102 and 0.124 nm^{-1} , and hence the *d*-spacings, or $d_{(10)}$ and $d_{(01)}$, are 61.6 and 50.7 nm. The angle between the two scattering vectors, 65° , gives the angle α , 115° , between two real lattice vectors. The *d*-spacings and the angle α , in turn, give magnitudes of real lattice vectors, $|a|$ and $|b|$, i.e., 68.0 and 55.9 nm, respectively. Furthermore, the domain spacing of layered matrix of S and I estimated by

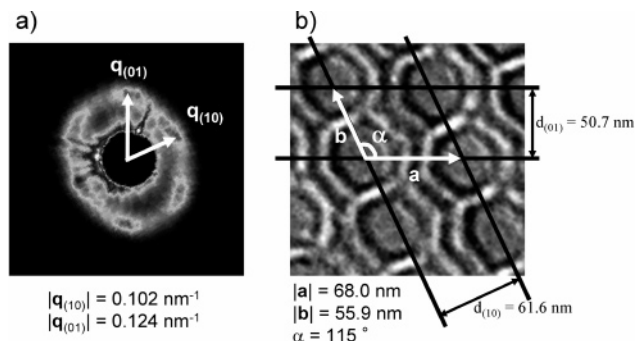


Figure 3. (a) Microbeam SAXS pattern and (b) the corresponding transmission electron micrograph for much narrower domain area of undeca21.

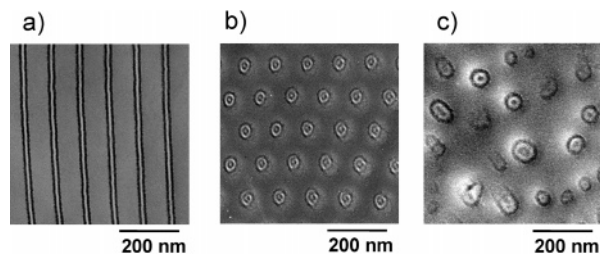


Figure 4. Transmission electron micrographs of hexablock terpolymers: (a) hexa64, (b) hexa75b, and (c) hexa88. Ultrathin sections were stained with OsO_4 and I_2 .

the transmission electron micrograph is ca. 16 nm, the value is again equivalent to that of the nonablock copolymer. Consequently, undeca21 is confirmed to form oblique packed cylinders-in-lamellae structure with hierarchical double periodicity. And because of oblique packing of P cylinders, matrix of I and S is split into three and five layers.

In turn experimental results for hexablock terpolymers are described in the following several paragraphs. Bulk structures of solvent-cast and annealed films of precursors were observed by TEM and SAXS methods (see the Supporting Information), and it was confirmed that diblock and quarter block copolymer precursors show bicontinuous structures, while triblock and pentablock ones exhibit lamellar ones. The domain spacing of S-I layers for pentablock, was determined as 18.0 nm.

Figure 4 compares transmission electron micrographs of three hexablock terpolymers. From Figure 4a, it is apparent that hexa64 forms lamellae-in-lamella structure which is composed of one thick P lamella and three thin I-S-I lamellae. Considering that undeca53 forms five-layered structure, it is evident that the difference in these structures is due to the difference in their primary molecular structures. The number of ways of block chain distribution was counted using the same method as adopted in a previous work,³⁷ and it was found that the relative fraction of the three-layered structure and the five-layered one formed by the hexablock terpolymer is 0.66 and 0.34; therefore, the latter actually could be expelled by the former. Figure 5 show a SAXS profile of hexa64, where integer-ordered peaks can be clearly recognized up to the ninth order, reflecting a highly ordered lamellar structure with a longer repeating distance, *D*, of 93.5 nm. From Figure 4b, hexa75b forms hexagonally packed cylinders composed of I and S in matrix of P component, where I and S domains are phase-separated concentrically into cylinders, so it can be called as coaxial cylindrical structure. In addition hexa87 forms I-S concentric spheres with four layers in matrix of P component as shown in Figure 4c, where I and S components are mostly separated into I-S-I core-shell structure; consequently, hexa87 forms an onionlike spherical structure with low ordering.

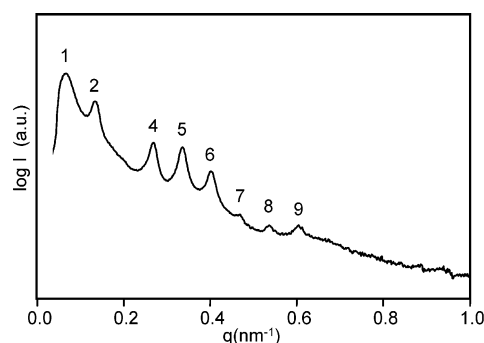


Figure 5. Small-angle X-ray scattering profile obtained from hexa64.

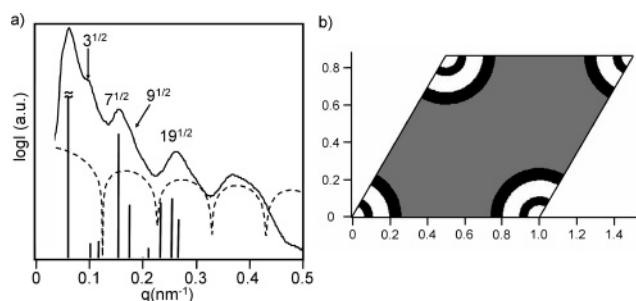


Figure 6. (a) SAXS profile (solid curve) obtained for hexa75b. The vertical bars represent the calculated intensities based on the coaxial cylindrical structure shown in part b, while a dashed curve denotes calculated "particle scattering" for four-circle coaxial cylinders composed of I and S. (b) Corresponding model for hexagonally packed coaxial cylinders. S, I, and P domains appear as white, black, and gray, and their electron density values are 0.565, 0.515, and 0.607 mol electron/cm³ respectively.

Figure 6a shows a regular SAXS intensity curve for hexa75b, where several peaks are observed at the relative magnitude of the scattering vectors of 1, 3^{1/2}, 7^{1/2}, 9^{1/2}, 19^{1/2}, etc. These values are typical reflection series from a hexagonally packed cylindrical structure, though several peaks are overlapped since the angular resolution was not satisfactory. The cylinder-to-cylinder distance, D_c , can be estimated to be 125 nm by using the relationship, $D_c = (4/3)^{1/2} 2\pi/|q_{10}|$ known for hexagonally packed cylinders where $|q_{10}|$, 0.0573 nm⁻¹, denotes the magnitude of the scattering vector for the first peak. Figure 6b exhibits the electron density profile for the cross section of the coaxial cylindrical structure assuming four-circle coaxial cylinders. At the bottom of Figure 6a the calculated relative diffracted intensities based on the unit cell in Figure 6b are exhibited, where electron densities for I, S, P are 0.515, 0.565, 0.607 mol electron/cm³, respectively. The calculated ones are again consistent with the observed relative intensity heights. In Figure 6a, the calculated "particle scattering" intensity for four-circle cylinders is shown as a dashed curve, where the outer diameter of cylinders determined by D_c , 31 nm, was used. From this curve, the diffracted intensities at $|q|$ of 4^{1/2} and 16^{1/2} are expected to be vanished, and it is quite consistent with the measured SAXS profile. Furthermore, Figure 7a demonstrates a microbeam SAXS pattern of hexa75b and the schematic drawing of the corresponding structure is in Figure 7b. The SAXS pattern reveals a 6-fold symmetry, which is consistent with the hexagonally packed cylinders. The d -spacing and the lattice constants for this hexagonal lattice were determined in the same manner as for undeca21, and they are as follows: $d_{(10)} = d_{(01)} = 110$ nm, $|a| = |b| = 127$ nm, $\alpha = 120^\circ$. $|a|$ and $|b|$ correspond to D_c and the obtained value is quite consistent with the one, 125 nm, from regular SAXS. These facts in the reciprocal lattice space are strong evidence to confirm the

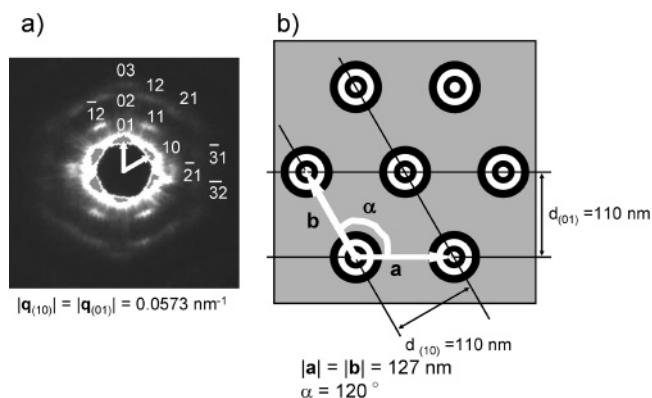


Figure 7. (a) Microbeam SAXS pattern and (b) the corresponding schematic structure of hexa75b.

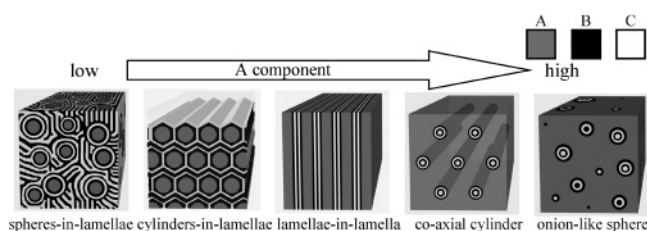


Figure 8. Schematic summary of composition-dependent morphological transition of multiblock terpolymers of A(BC)_nBA type and A(BC)_nB type. Three contrasts, i.e., gray, black, and white regions, correspond to A, B, and C domains, respectively.

hierarchical structure with hexagonally packed coaxial cylinders in matrix.

Undecablock terpolymers and hexablock ones can be regarded to show essentially the same structural feature from the viewpoint of forming nanophase-separated structure, referring to the similarity between ABA triblock and AB diblock copolymers. Therefore, morphological transition of hierarchical structures was commonly explained for undecablock and hexablock terpolymers. An undecablock terpolymer of the P(IS)₄IP type exhibits spheres-in-lamellae structure when P occupies 8% and terpolymers of the same type show cylinders-in-lamellae, lamellae-in-lamella structures if volume percent of P component are 21% and 53%. In turn, hexablock terpolymers with P of 64%, 75%, and 87% represents a lamellae-in-lamella structure, coaxial cylinders in matrix, and an onionlike spherical structure in matrix, respectively. To summarize these results, Figure 8 schematically shows phase behavior for multiblock terpolymers of A(BC)₄BA and A(BC)₂B type. If we focus on A(gray) domain, it transforms from sphere into cylinder, lamella and finally into matrix with increasing the fraction of A component, while domains of B—C mixed phase transform from matrix into lamella, cylinder and sphere with keep possessing alternating layered structure. Thus, the morphological transition manner of hierarchical structures formed by multiblock terpolymers is essentially analogous to the transition of AB and ABA block copolymers.

In summary, the morphological features for two types of multiblock terpolymers, i.e., P(IS)₄IP and P(IS)₂I were investigated. Undecablock terpolymers with lower volume fractions of P component and hexablock terpolymers with higher volume fractions of P have been successfully prepared and used. From morphological observation by using TEM and SAXS methods, it has been found these terpolymers form new hierarchical nanophase-separated structures, i.e., spheres-in-lamellae, cylinders-in-lamellae, and lamellae-in-lamella structures, hexagonally packed coaxial cylinders in matrix, and an onionlike spherical

structure. If attention is paid on the domain shape of P component, it transforms from spheres to cylinders, to lamellae, and finally to matrix with increasing its volume fraction. Thus, we have found that morphological transition takes place obeying the conventional rule applied for AB and ABA block copolymers with keeping hierarchical nature.

Acknowledgment. The authors thank Dr. S. Arai at the Center for Ecotopia Science Institute in Nagoya University for his help in obtaining the TEM. This work was partially supported by the 21st Century COE program entitled "The Creation of Nature Guided Materials Processing" and Y.M. expresses thanks for the support.

Supporting Information Available: Text and figures showing morphological observations for precursors of undecablock and hexablock terpolymers, which were carried out in detail. This material is available free of charge via the Internet at <http://pubs.acs.org>.

References and Notes

- (1) Matsuo, M.; Sagae, S.; Asai, H. *Polymer* **1969**, *10*, 79.
- (2) Leibler, L. *Macromolecules* **1980**, *13*, 1602.
- (3) Ohta, T.; Kawasaki, K. *Macromolecules* **1986**, *19*, 2621.
- (4) Matsushita, Y.; et al. *Macromolecules* **1990**, *23*, 4313.
- (5) Park, S.; et al. *Macromolecules* **2003**, *36*, 4662.
- (6) Hajduk, D. A.; et al. *Macromolecules* **1996**, *29*, 1473.
- (7) Gido, S. P.; et al. *Macromolecules* **1993**, *26*, 2636.
- (8) Stadler, R.; et al. *Macromolecules* **1995**, *28*, 3080.
- (9) Mogi, Y.; et al. *Macromolecules* **1993**, *26*, 5169.
- (10) Matsushita, Y. *J. Polym. Sci., Part B* **2000**, *38*, 1645.
- (11) Nakazawa, H.; Ohta, T. *Macromolecules* **1993**, *26*, 5503.
- (12) Matsen, M. W. *J. Chem. Phys.* **1998**, *108*, 785.
- (13) Avgeropoulos, A.; et al. *Macromolecules* **1997**, *30*, 5634.
- (14) Noro, A.; et al. *Macromolecules* **2004**, *37*, 3804.
- (15) Hadjichristidis, N.; et al. *Macromolecules* **1993**, *26*, 5812.
- (16) Matsushita, Y.; et al. *Polymer* **1997**, *38*, 149.
- (17) Alward, D. B.; et al. *Macromolecules* **1986**, *19*, 215.
- (18) Thomas, E. L.; et al. *Nature (London)* **1988**, *334*, 598.
- (19) Spontak, R. J.; Smith, S. D. *J. Polym. Sci.: Part B* **2001**, *39*, 947.
- (20) Matsushita, Y.; et al. *Polymer* **1994**, *35*, 246.
- (21) Wu, L.; et al. *Macromolecules* **2004**, *37*, 3360.
- (22) Zhu, Y.; et al. *Macromolecules* **2003**, *36*, 148.
- (23) Takano, A.; et al. *Macromolecules* **2003**, *36*, 3045.
- (24) Yamauchi, K.; et al. *Macromolecules* **2003**, *36*, 6962.
- (25) Takano, A.; et al. *J. Polym. Sci.: Part B* **2005**, *43*, 2427.
- (26) Hayashida, K.; et al. *Macromolecules* **2006**, *39*, 9402.
- (27) Ruokolainen, J.; et al. *Science* **1998**, *280*, 557.
- (28) Ruokolainen, J.; ten Brinke, G.; Ikkala, O. *Adv. Mater.* **1999**, *11*, 777.
- (29) Ikkala, O.; ten Brinke, G. *Science* **2002**, *295*, 2407.
- (30) Asari, T.; et al. *Macromolecules* **2005**, *38*, 8811.
- (31) Asari, T.; et al. *Macromolecules* **2006**, *39*, 2232.
- (32) Erukhimovich, I. Y.; Smirnova, Y. G.; Abetz, V. *Polym. Sci. Ser. A* **2003**, *45*, 1093.
- (33) Nagata, Y.; et al. *Macromolecules* **2005**, *38*, 10220.
- (34) Nap, R.; Erukhimovich, I.; ten Brinke, G. *Macromolecules* **2004**, *37*, 4296.
- (35) Smirnova, Y.; ten Brinke, G.; Erukhimovich, I. Y. *J. Chem. Phys.* **2006**, *124*, 054907.
- (36) Nap, R.; et al. *Macromolecules* **2006**, *39*, 6765.
- (37) Masuda, J.; et al. *Phys. Rev. Lett.* **2006**, *97*, 098301.
- (38) Hayashida, K.; et al. *Macromolecules* **2006**, *39*, 4869.

MA070155S